

STRUCTURAL APPLICATIONS OF NUCLEAR SPIN-LATTICE RELAXATION TIMES

David M. Doddrell

School of Science, Griffith University, Nathan, Queensland, 4111
Australia

Abstract - The structural utility of three mechanisms of nuclear spin relaxation are considered. Examples illustrating the applicability of nuclear-nuclear dipolar relaxation in determining molecular microdynamics and solution geometry are presented. The use of spin-rotation relaxation to determine barriers to CH₃ groups rotations and an example of quadrupole relaxation of deuteriums to probe molecular motion are discussed.

An experimental method for determining relaxation times is briefly analysed.

INTRODUCTION

Structural applications of nuclear magnetic resonance spectroscopy have usually only involved chemical shift (σ) and coupling constant (J) considerations. The reasons for this are manifold, the main ones include: (a) most commercial instruments have been CW-based and the measurement of any other magnetic resonance parameter besides σ or J is difficult, and (b) the technology for the measurement of the spin-lattice (T_1) relaxation time of a single resonance line in a multi-line spectrum has only been available since the development of FT based spectrometers. The major break-throughs here being the cheap cost of on line mini-computers, but more importantly, the development of the FFT algorithm. There are exceptions to the above generalizations, the major one being structural investigations using the nuclear Overhauser effect (NOE).

In this lecture I plan to review briefly and descriptively the theoretical basis of nuclear spin relaxation and discuss the applications of three spin relaxation mechanisms in structural chemistry. It is not my intention to present an exhaustive review.

Whereas chemical shifts and coupling constants can be related to the electronic environment of the nucleus and the conformation of the molecule, the nuclear relaxation times, because of their very nature, are related to the time-dependent processes acting on the molecule. Just as the observation of the nmr spectrum requires the application of a time-dependent magnetic field to cause nuclear transitions, nuclear spin relaxation arises because of time-dependent magnetic fields arising from the lattice. Without spin relaxation, the observation of the nmr spectrum would be impossible.

We will consider the structural utility of three mechanisms of spin relaxation. In all cases T_1 can be related to the square of the strength of the coupling between the spin system and lattice and the characteristic time constant (τ) of the time-dependency of the coupling, that is

$$T_1^{-1} = \bar{E}^2 \tau \quad (1)$$

where \bar{E}^2 is the average of the square of the interaction energy¹.

From a structural standpoint, the dipole-dipole interaction is the most useful as it can be related to the distance of separation of the interacting nuclei and may yield information on the solution geometry. In a dilute solution of a rigid molecule, the time-dependence arises from the rotational reorientation of the molecule. In the molecular reference frame the dipole-dipole coupling is time invariant but in the laboratory axis, the axis system in which the nmr measurement is made, the coupling is time-dependent. The relaxation rate of nucleus I from dipolar coupling to nucleus S is given simply, in most cases, by the expression¹

$$T_1^{-1} = \frac{\hbar^2 \gamma_S^2 \gamma_I^2}{r_{IS}^6} \tau_c = \frac{k \tau_c}{r_{IS}^6} \quad (2)$$

where \hbar , γ_S , and γ_I are constants, τ_c is the correlation time for rotational reorientation of the molecule, and r_{IS} the internuclear separation. If I and S are the same nuclear species (e.g. both protons) (2) becomes

$$T_1^{-1} = \frac{3}{2} \frac{\hbar^2 \gamma_H^4}{r_{IS}^6} \tau_c \quad (3)$$

and if more than one proton is involved in causing the relaxation of H_I (3) becomes

$$T_1^{-1} = \frac{3}{2} \hbar^2 \gamma_H^4 \sum_j r_{IS_j}^{-6} \tau_{IS_j} \quad (4)$$

The relaxation rate of a protonated ^{13}C nucleus by the attached protons is given by²

$$T_1^{-1} = N \frac{\hbar^2 \gamma_C^2 \gamma_H^2}{r_{CH}^6} \tau_c = NK\tau_c \quad (5)$$

r_{CH} is a well-known constant, 1.09\AA , N is the number of attached protons, and K a constant, $3.56 \times 10^{10} \text{ s}^{-2}$. We will see later that equation (5) can be employed in two different ways as a structural probe. Firstly, if N is known (from say a single-frequency decoupled ^{13}C spectrum) measurement of T_1 yields a direct measurement of τ_c and hence the molecular microdynamics can be probed. Also this technique allows an experimental determination of τ_c which may be used in other relaxation studies. Secondly, if τ_c is constant (as in a rigid molecule), a T_1 measurement may be used to determine the number of attached protons. This is a very useful technique for the many cases where proton single-frequency off-resonance decoupling does not yield a clear-cut answer.

The second mechanism we will consider is quadrupolar relaxation. If the nucleus has a spin quantum number $I > 1/2$ and the electric field gradient is non-zero at the nucleus, the nuclear spin couples with the quadrupole and the interaction is time modulated by the molecular reorientation causing spin relaxation. For a spin 1 nucleus (e.g. ^{14}N or ^2H) T_1 is given, under certain conditions, by¹

$$T_1^{-1} = \frac{3}{2} \left(\frac{e^2 q Q}{2\hbar} \right)^2 \tau_c \quad (6)$$

$(e^2 q Q / 2\hbar)$ is the quadrupole coupling constant and may be either measured from the solid state nmr spectrum or, in some cases, by nuclear quadrupole resonance spectroscopy. The main structural utility of this mechanism is probably in applications of ^2H nmr because in this case the quadrupole coupling constant (180-200 kHz) is independent of the electronic environment of the deuterium. This method also allows the molecular microdynamics to be probed. Of course, if τ_c is known (from say a ^{13}C T_1 measurement), measurement of T_1 of a quadrupolar nucleus allows the quadrupole coupling constant to be measured in solution and hence the electronic structure can be probed. There have been few reports so far using the latter idea.

The last mechanism I wish to discuss is spin rotation relaxation. The nuclear spin couples to the rotational angular momentum of the molecule and as the molecule rotates (or if there is internal motion) the coupling is time modulated causing nuclear relaxation. The main structural applications employing the spin rotation interaction have been in measuring very low energy barriers to CH_3 group rotations³.

Measurement of Relaxation Times

In discussing spin relaxation time measurements it is more convenient to consider the response of the bulk magnetization \underline{M} induced in the sample by the applied static field to applied radio-frequency pulses of a given duration. Initially, \underline{M} is aligned with the field in the z' -direction; we speak of 90° pulses which tip \underline{M} into the $x'-y'$ plane and 180° pulses which rotate \underline{M} to the $-z'$ direction.

The most commonly employed procedure for measuring T_1 values is the 180° - τ - 90° (inversion-recovery) pulse sequence, (Figure 1)¹. Firstly, a 180° pulse applied along the x' axis flips the magnetization \underline{M} to the $-z'$ axis. Spin-lattice (longitudinal) relaxation now occurs and, if at time τ seconds after the 180° pulse, a 90° pulse is applied also along the x' axis, $\underline{M}(\tau)$ is nutated onto the y' axis and a signal is detected. The strength of the signal is a simple function of τ and T_1

$$M(\tau) = M_0 (1 - 2e^{-\tau/T_1}) \quad (7)$$

where M_0 is the equilibrium amplitude.

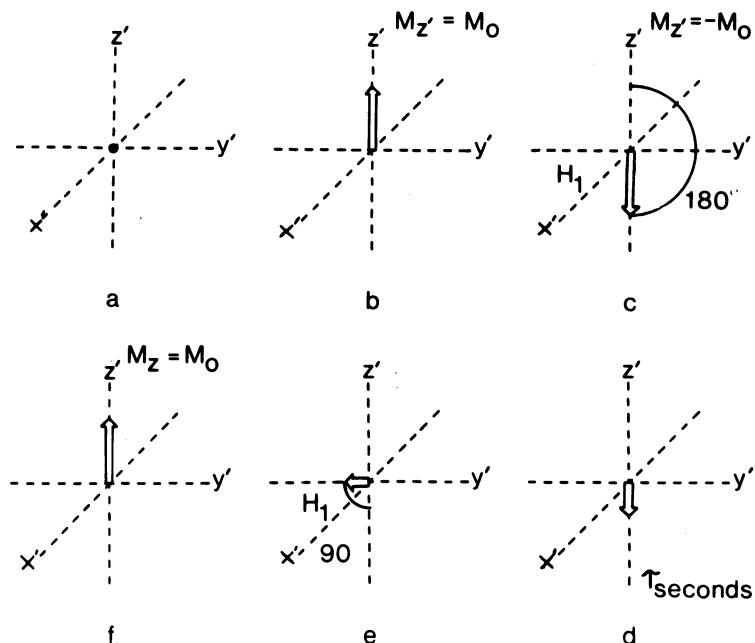


Figure 1 - Representation of the 180° - τ - 90° pulse sequence for measuring T_1 values. a \rightarrow b: Buildup of the magnetization after the application of the static magnetic field. b \rightarrow c: Application of a 180° pulse and inversion of the equilibrium magnetization M_0 . d: After a wait time τ seconds. The case $\tau < T_1 \ln 2$ is shown. d \rightarrow e: Application of the 90° observation pulse. f: Completely recovered magnetization after a long wait interval. See reference 1.

In practice, equation (7) is rearranged into the form

$$\ln(A_\infty - A_\tau) = \ln(2A_\infty) - \tau/T_1, \quad (8)$$

where A_τ is the initial amplitude of the free induction decay (FID) following the 90° pulse and A_∞ is the limiting value of A_τ for a very long interval between the 180° and 90° pulses. T_1 is determined from the slope of the plot of $\ln(A_\infty - A_\tau)$ versus τ for a series of spectra recorded at different τ settings. The behaviour of each line in a spectrum can be monitored if the Fourier transformation is taken following the 90° pulse. If two nuclei have different T_1 values, the intensity of their resonances will have a different dependence on τ . A resonance line will appear inverted, nulled, or positive (with respect to the normal spectrum) depending on whether τ is smaller, equal to, or larger than $T_1 \ln 2$, respectively. Figure 2 shows a set of relaxation spectra obtained for the olefinic carbon of $\text{Pd}(\text{AA})_2$ (AA = acetylacetonate) for different τ values. Note the inversion of the signal (relative to normal spectrum) for $\tau < T_1 \ln 2$, the null at $\tau 0.7\text{s}$, and for larger τ values, a positive signal. A data plot is also shown⁴.

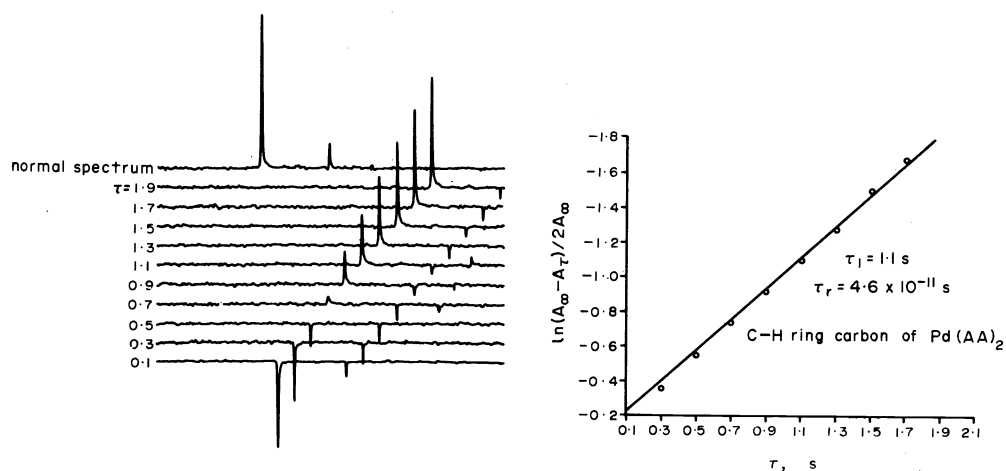


Figure 2 - A series of relaxation spectra for the CH ring carbon resonance from a solution of Pd(AA)₂ in CDCl₃. 150 pulses were collected using a recycle time of 7.5s. τ (s), the time between 180° and 90° pulses, is shown on the diagram. 8K data points were used. A data plot is shown.

Reprinted with permission from Chem.Phys.Letts. **40**, 142 (1976).

Application of ¹³C-¹H dipole-dipole relaxation to study molecular microdynamics

One of the first applications of Fourier transform relaxation time measurements involved using ¹³C relaxation times of protonated carbons to probe the microdynamics at local sites in a complex molecule^{2,5}. The power of this technique for this type of study can be appreciated by inspecting the data in Figure 3 which show a set of relaxation spectra for 1-octanol. Consider the peaks at either end of the spectrum. The most downfield resonance arises from the hydroxylated carbon and the most upfield from the terminal methyl carbon. They show a markedly different dependence on τ , the time between the 180° and 90° pulses. The CH₃ carbon resonance is still inverted when the CH₂OH carbon resonance has returned to the same phase as the equilibrium spectrum demonstrating that the CH₃ carbon has a much longer T₁ than the CH₂OH carbon. The opposite conclusion would have been reached if the relative T₁'s had been based solely on considerations of numbers of attached protons. This can be readily understood by writing the effective correlation time τ_{eff} affecting T₁ as

$$\tau_{\text{eff}}^{-1} = \tau_{\text{C}}^{-1} + \tau_{\text{G}}^{-1} \quad (9)$$

where τ_{C} is the correlation time for the overall rotational motion and τ_{G} the effective correlation time for internal motion of the groups. When $\tau_{\text{G}} < \tau_{\text{C}}$, τ_{G} dominates τ_{eff} . Thus if τ_{G} is different for two carbons and both τ_{G} 's are such that $\tau_{\text{G}} < \tau_{\text{C}}$, the carbon with the fastest motion will have the longest T₁.

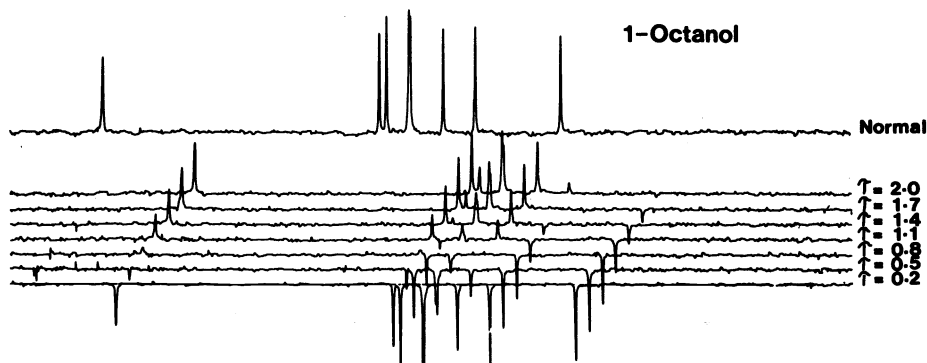
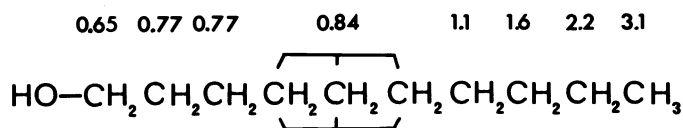
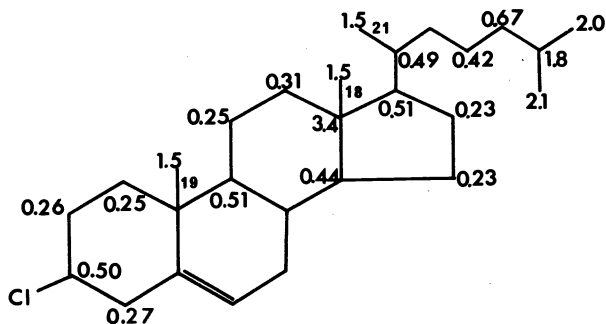


Figure 3 - A set of relaxation spectra for ^{13}C resonances in 1-octanol. The τ values are in seconds.

This is apparently what is happening in the case of 1-octanol; the hydroxylated end will be moving more slowly because of hydrogen bonding whereas the CH_3 group end will be free to "wiggle". There should therefore be a gradual increase in T_1 moving from the hydroxylated end to the CH_3 group end. Results for 1-decanol⁵ demonstrating that this is so are shown in Figure 4.



a



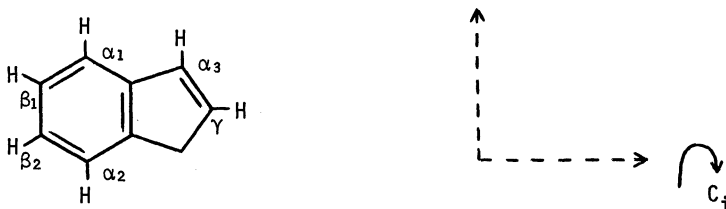
b

Figure 4 - ^{13}C T_1 (s) values for the various positions in (a) 1-decanol, and (b) cholesterol chloride. See references 5 and 6.

Segmental motion and relaxation time measurements, in general, are very useful as an aid for assigning the ^{13}C spectrum of a complex molecule. The principles involved are readily illustrated by data for cholesteryl chloride (Figure 4). Note the following⁶:

- (1) Because the backbone is rigid, protonated carbons on the backbone have $T_1 \propto N^{-1}$. For example, the T_1 of the CH_2 carbons C-1, C-2, ..., C-15, C-16 are half the T_1 of the CH carbons C-3, C-9, C-13.
- (2) Non-protonated carbons have the longest T_1 's, e.g. 3.4s for C-13, twice as long as for any other carbon in the molecule.
- (3) The methyl groups, C-18 and C-19, have T_1 's lengthened by fast rotation of the CH_3 group. In fact, it may be shown theoretically that the T_1 of CH_3 carbons should be three times that of the CH backbone carbons. Within experimental error it is.
- (4) The T_1 's of carbons on the hydrocarbon side-chain attached at C-17 clearly show the effects of segmental motion of the chain, the T_1 of C-25, a mono-protonated carbon, is more than three times that of the T_1 of a corresponding carbon on the backbone. The T_1 's of C-27 and C-26 also clearly show the effects of segmental motion.

The utility of T_1 's as an assignment aid are readily demonstrated in assigning the ^{13}C spectrum of even the simplest carbon compound. Consider indene. It is not apparent from chemical shift considerations what the correct assignments are for the 6 C-H carbons. In fact, the assignments reported in the literature based solely on these considerations appear to be incorrect⁷. The ^{13}C - ^1H coupled spectrum is of some use but does not provide the full answer. If we draw and number the molecule as shown below



then it can be readily appreciated that motion about the C_i rotation axis should (a) affect the relaxation rate of the α -carbons the most, (b) slightly lengthen the T_1 of the β -carbons, and (c) have no effect on the T_1 of C_γ because for this carbon rotation about this axis does not change the orientation of the C-H vector. Thus, if relaxation spectra are recorded for this compound, the C-H resonances should be blocked into one group of three, a group of two, and one much longer than the rest. This behaviour is evident in the spectra shown in Figure 5.

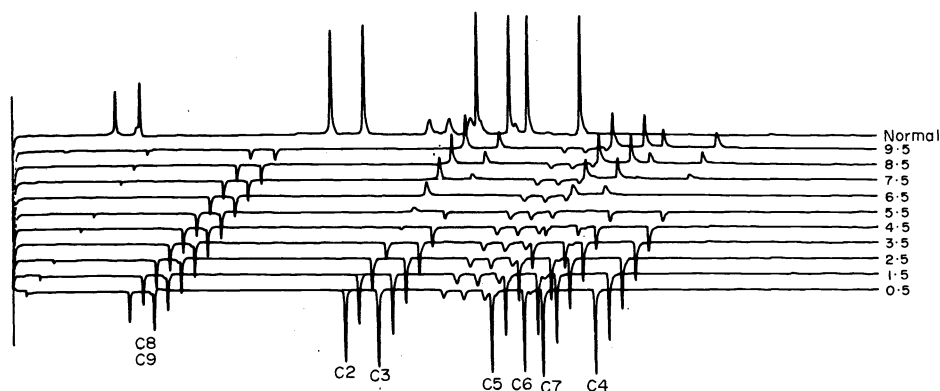


Figure 5 - A set of relaxation spectra for the ^{13}C resonances in indene showing the different behaviour of the resonances as a function of τ (in seconds).

Probably the most dramatic illustration of the use of the effects of segmental motion as an assignment aid⁶ is its use in assigning the ^{13}C spectrum of the tetrasaccharide stachyose (Figure 6). Although it is quite a simple matter to divide the resonances into those arising from the fructofuranose, glucopyranose, and galactopyranose rings, it is not possible to differentiate between the resonances of the two galactopyranose rings using conventional procedures. However, from a consideration of the structure (Figure 6), it can be seen that one galactopyranose ring is terminal and is attached to the rest of the molecule by means of a $-\text{O}-\text{CH}_2-$ linkage. Thus, it may have faster internal reorientation and measurably longer ^{13}C T_1 values than the other rings. Examination of a relaxation spectrum (Figure 7) of stachyose with τ 0.34s reveals that the already identified galactose resonances can indeed be divided into two sets on the basis of appreciably different T_1 values. When τ is 0.34s, one set of resonances is nulled ($T_1 \approx 0.5\text{s}$), while the other set is positive ($T_1 < 0.5\text{s}$). The nulled resonances can thus be assigned to the terminal galactose ring. It should be noted that it is not necessary to determine the actual T_1 's of the carbons in order to make assignments. Comparison of intensities within a single relaxation spectrum is often sufficient.

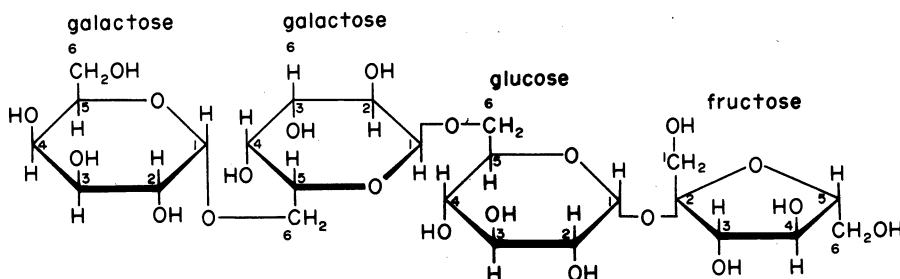


Figure 6 - Structure of Stachyose.

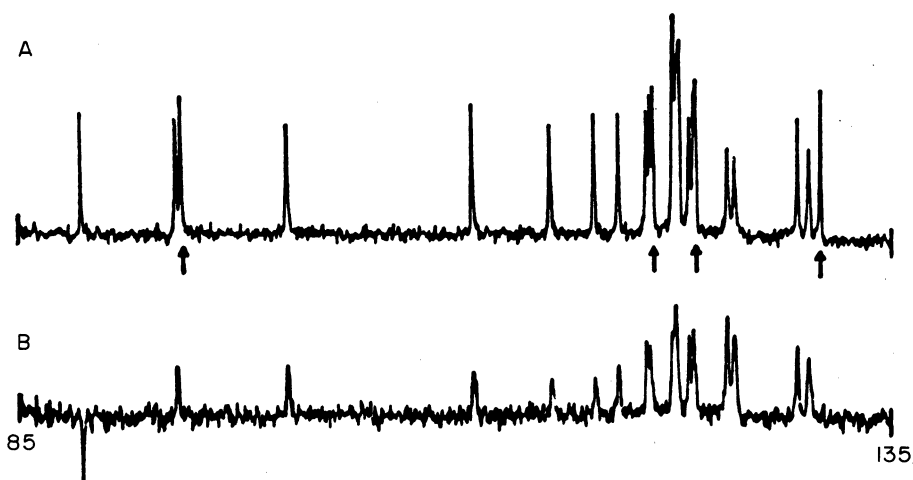


Figure 7 - Proton-decoupled ^{13}C nmr spectra of 0.5M stachyose at 65° obtained at 15.08 MHz. (A) Normal spectrum after 256 pulses. (B) Relaxed spectrum with τ 0.34s after 512 pulses. Arrows in the top spectrum indicate terminal galactose resonances identified from the relaxed spectrum.

Reprinted with permission from J. Amer.Chem.Soc. 93, 2778 (1971).
Copyright by the American Chemical Society.

There have been many papers published recently on ^{13}C relaxation studies of large molecular weight "biologically relevant" molecules. Except for a few notable exceptions, these studies have been concerned with measuring the T_1 of all the resolved resonances and analysing descriptively which groups are moving fast or slow, or whether there is indeed any segmental motion at all. It is probably fair to say at this stage of the development of the technique, that very little biochemically important information has been uncovered although the potential is clearly evident. One of the first applications of the method was to the work-horse of biochemical nmr studies, ribonuclease A⁸. A set of relaxation spectra for this protein are shown in Figure 8. It is readily apparent that there are differences in the T_1 of the carbons; the carbonyls have, as expected, the longest T_1 while the protonated rigid α - and β -carbons have the shortest. The very sharp peak at 153.7 ppm upfield from CS_2 arises from the ϵ -carbon of the ten lysine residues. They have a very long T_1 independent of whether the protein is native or denatured clearly demonstrating the importance of segmental motion. As expected, the spectrum becomes much sharper when the protein is denatured (Figure 9) and there is a marked increase in the relaxation times (Table 1).

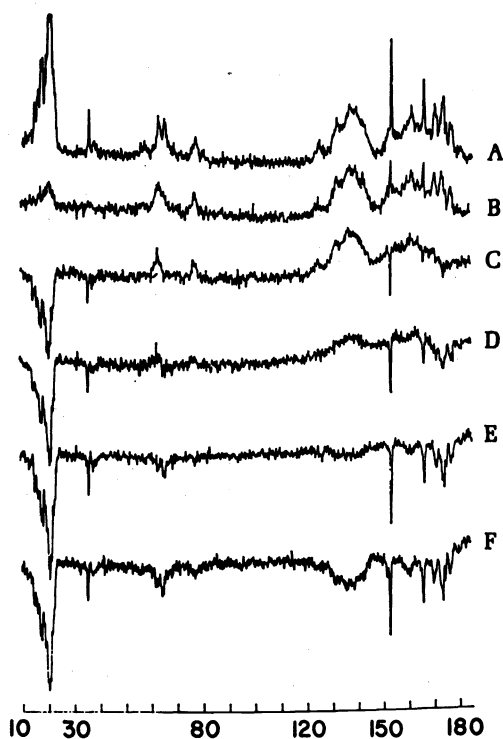


Figure 8 - Proton-decoupled ^{13}C spectra of 0.019M ribonuclease A at 45° , pH 6.53, and 15.08 MHz.

(A) normal spectrum. (B)-(F) relaxed spectra. τ is in ms. (B) 336.9, (C) 82.3, (D) 39.8, (E) 18.6, (F) 7.96.

Reprinted with permission from *J.Amer.Chem.Soc.* 93, 545 (1971).
Copyright by the American Chemical Society.

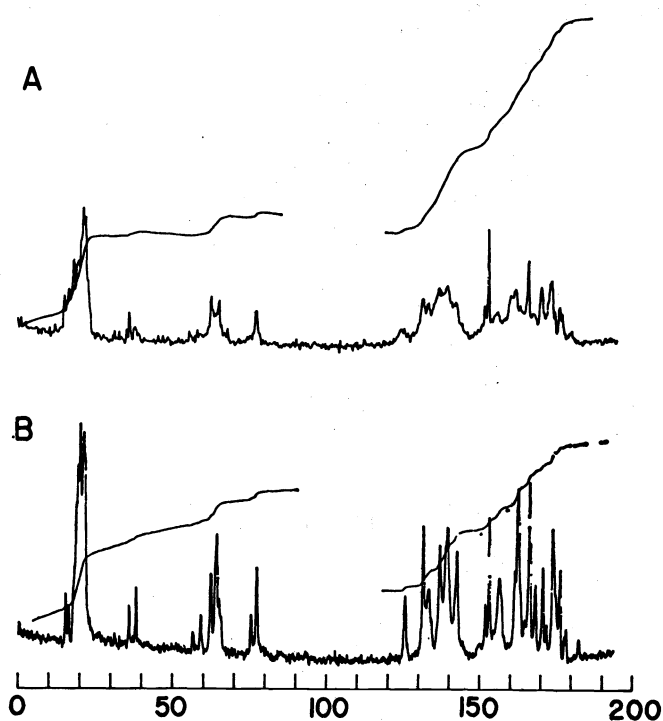


Figure 9 - Proton-decoupled ^{13}C nmr spectra of ribonuclease A at 45° and 15.08 MHz. Horizontal scale is in ppm upfield from CS_2 . (A) 0.017M native protein at pH 4.12. (B) 0.015M denatured protein at pH 1.46.

Reprinted with permission from J. Amer. Chem. Soc. 93, 545 (1971).
Copyright by the American Chemical Society.

TABLE 1 Some Carbon-13 Spin-Lattice Relaxation Times and Rotational Correlation Times in Aqueous Ribonuclease A.^a

Type of Carbon	Native Protein ^b		Denatured Protein ^c	
	T_1 (ms)	τ_c (ns)	T_1 (ms)	τ_c (ns)
α - carbons	42	30	120	0.40
β - carbons	40	30	99	0.48
ϵ - carbons of LYS	330	0.070	306	0.076

^aObtained for 0.019M protein at 45° and 15.08 MHz.

^bpH 6.51.

^cpH 1.64.

It is clear from the above discussion that spectra of native proteins are quite broad and even the large chemical shift range expected for ^{13}C nuclei at high (super-conducting) field strengths will not enable many protonated carbons to appear as well-resolved resonances. However, as Allerhand has pointed out⁹, because of the r^{-6} dependence of T_1^{-1} , in native proteins non-protonated carbon resonances will still be very sharp (width 1 Hz) and because instrument techniques are available to remove all resonances except those from non-protonated carbons (Figure 10), it is possible to use these types of carbons as a probe for

studying the solution properties of proteins. For such studies to be undertaken the resonance lines have to be assigned to specific carbons of a specific residue of the protein. Information available from relaxation studies is invaluable for this task. Consider the non-protonated carbons of three common amino-acid residues of proteins (Figure 11). In H_2O as solvent, C_{δ_2} of TRP has one proton, C_{E_2} of TRP two protons, C_{ϵ} of TYR and C_{γ} of TRP three protons, C_{γ} of TYR and C_{γ} of HIS four protons attached to the adjacent atom(s) while in D_2O as solvent, C_{ϵ} of TYR, C_{γ} of HIS, and C_{E_2} of TRP have this number reduced by one. Thus, there should be variations in the T_1 's because of variations in the number of adjacent protons and also on changing the solvent from H_2O to D_2O . Relaxation spectra⁹ of horse heart cyanoferri-cytochrome C (Figure 12) clearly show this to be the case and allow the assignments of TRP-59 C_{E_2} and TRP-59 C_{δ_2} to be made. Assignment of the resonances of these carbons would be "impossible" to do by conventional techniques.

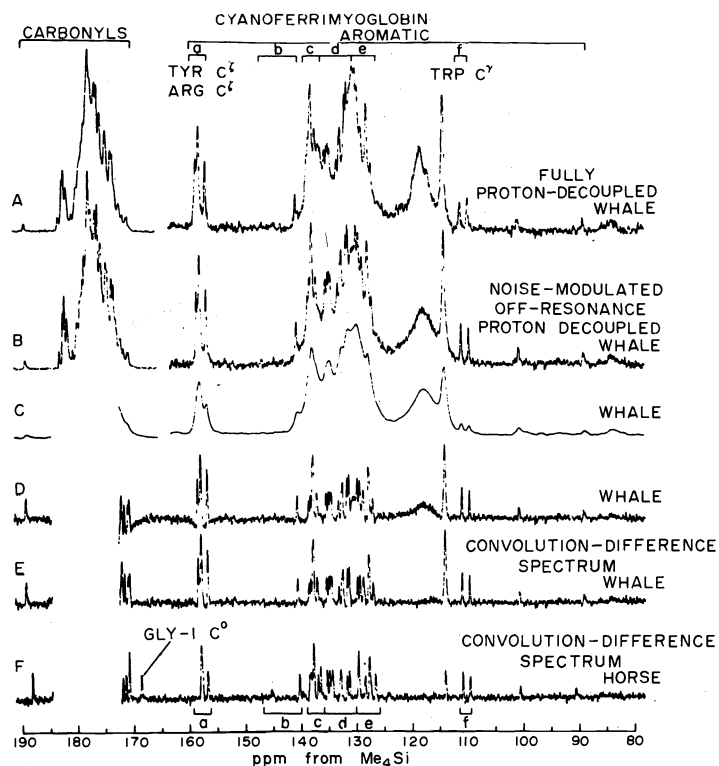


Figure 10 - Convolution-difference ^{13}C spectrum obtained from the fully proton-decoupled and noise off-resonance proton-decoupled spectra of 8.8 mM sperm whale cyanoferri-myoglobin in H_2O . For further details see reference 9. Reprinted with permission from *JBiol.Chem.* 250, 6385 (1975).

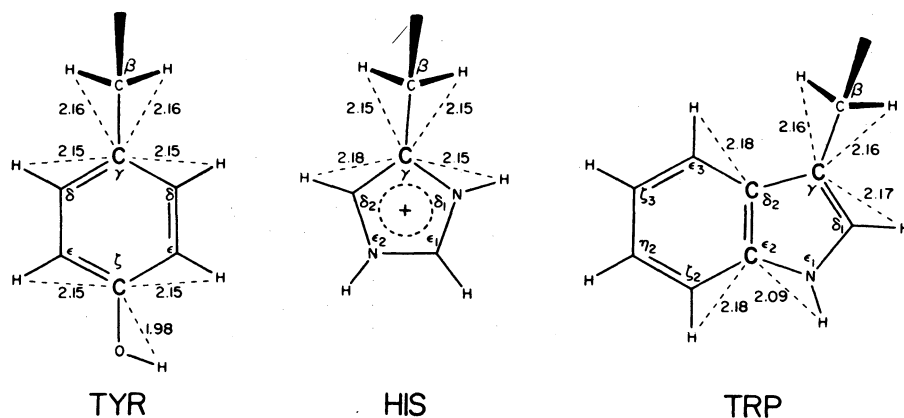


Figure 11 - Estimated distance of non-protonated aromatic carbons in TYR, HIS, and TRP. See reference 9.

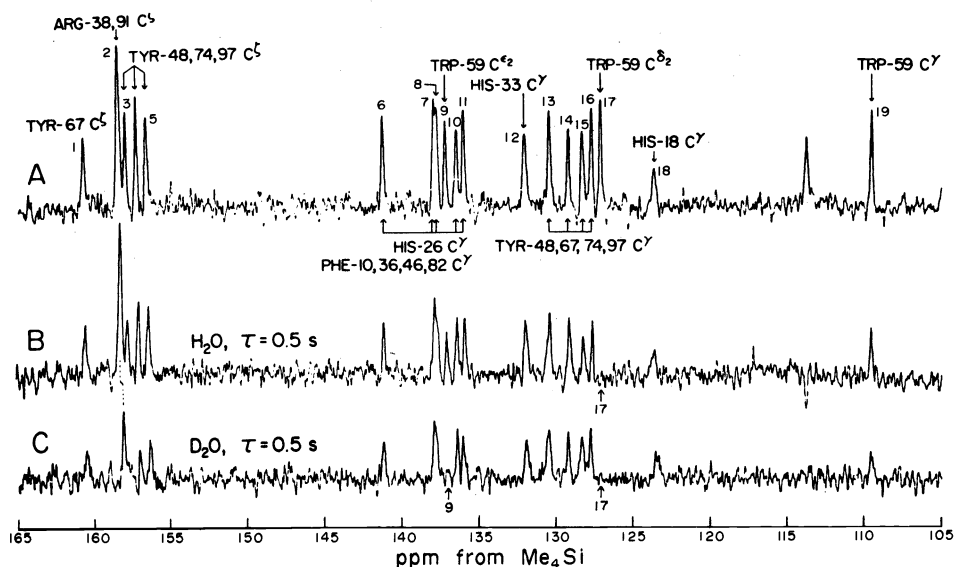


Figure 12 - Aromatic region in the convolution-difference ^{13}C spectra of 15 mM horse heart cyano-ferricytochrome C. (A) normal spectrum. (B) in H_2O , $\tau = 0.5\text{ s}$. (C) in D_2O , $\tau = 0.5\text{ s}$.

Reprinted with permission from J.Amer.Chem.Soc. 97, 223 (1975).
Copyright by the American Chemical Society.

Proton Relaxation Studies in Structural Analysis

(a) Of Paramagnetic Molecules

Although the theory of electron-nuclear dipole-dipole relaxation is more complicated than the corresponding nuclear-nuclear relaxation, the technique of adding paramagnetic line broadening agents has proven quite successful in structural chemistry¹⁰. A complete review is outside the scope of this lecture and there is, as well, insufficient time to consider this aspect of spin relaxation in any detail. Nevertheless, it is useful to consider a few examples to illustrate the technique. The contribution to T_1 of nucleus N from dipolar coupling to S unpaired electrons located on a metal ion is, under suitable conditions, given by

$$T_1^{-1} = \frac{2}{15} \frac{\gamma_e^2 \gamma_N^2 \hbar^2 S(S+1)}{r_{MN}^6} \{3\tau_S + \frac{7\tau_S}{1 + \omega^2 \tau_S^2}\} \quad (10)$$

where τ_S is an effective correlation time and r_{MN} the separation between the metal ion and the nucleus. Concanavalin A (Con A) binds Zn^{2+} , Co^{2+} and Mn^{2+} at one site S_1 and Ca^{2+} ions at another site S_2 . When metal ions are bound to the protein, the protein binds saccharides. However, there is quite a marked difference in the binding constants of α and β anomers with the α form bound much more tightly. ^{13}C T_1 measurements by Brewer and co-workers¹¹ of α - and β -methyl D-glucopyranoside bound to the Mn^{2+} derivative of Con A demonstrate that the α and β anomers have quite different binding orientations. Figure 13 shows the binding orientations and the quite fine detail that can be deduced using paramagnetic probes.

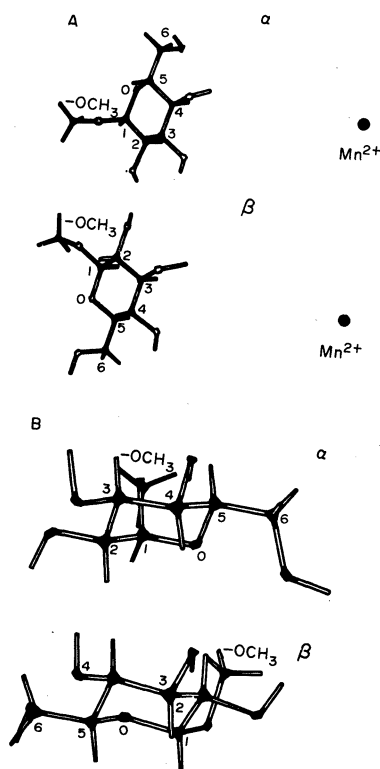


Figure 13 - Binding orientations of α - and β -methyl-D-glucopyranoside relative to the transition-metal ion site in Con A illustrated in (A) as a side view with the Mn^{2+} ion in the plane of the paper and (B) a front view as seen from the Mn^{2+} ion. Reprinted with permission from *Biochemistry*, **12**, 4454 (1973). Copyright by the American Chemical Society.

Another result⁴ worth discussing as it may lay the groundwork for a method of probing the solution geometry of discrete paramagnetic molecules also involves application of equation (10). Previous attempts to use this equation in solving structural problems have been hampered because τ_S was unknown. For a discrete molecule a simple solution to this problem is provided by measuring the ^{13}C T_1 of a suitable protonated carbon in the diamagnetic analogue as now $\tau_S = \tau_C$. As an example, consider methyl proton relaxation in the series of metal acetylacetonates $M(AA)_n$, $M = Cu(S = 1/2)$, $Cr(S = 3/2)$, $Fe(S = 5/2)$ and $VO(S = 1/2)$. τ_C can be measured from the T_1 of the C-H carbon of the Pd derivative. Here $T_1 = 1.1s$, yielding $\tau_C = 4.6 \times 10^{-11}s$. Using this value of τ_C and the X-ray determined distance of 4.8 Å for r_{M-H} of the CH_3 protons yield the theoretical T_1 values given in Table 2. There is excellent agreement with the experimental values suggesting the method may be useful for probing the solution geometry of paramagnetic molecules, in general.

TABLE 2 Calculated and Experimental T_1 's of the CH_3 Protons in Some $\text{M}(\text{AA})_n$ Complexes. τ_C has been taken as that in the corresponding diamagnetic compound. $n = 2$, $\tau_C = 4.6 \times 10^{-11}\text{s}$ ^a; $n = 3$, $\tau_C = 5.5 \times 10^{-11}\text{s}$ ^b

Metal	S	$T_1(\text{Exp})$	$T_1(\text{Cal})$
Fe($n = 3$)	5/2	0.34	0.30
Cr($n = 3$)	3/2	0.68	0.70
Cu($n = 2$)	1/2	3.6	4.2
VO($n = 2$)	1/2	4.2	4.2

^aBased on data for $\text{Pd}(\text{AA})_2$.

^bBased on data for $\text{Co}(\text{AA})_3$.

(b) Diamagnetic Molecules

The potential use of proton T_1 studies in structural chemistry has by no means been realized although the power of the method is clearly evident. I will speak about three such applications.

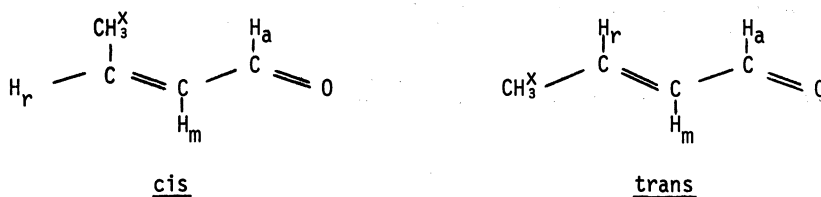
Hall and Preston in 1972 clearly illustrated the utility of ^1H T_1 studies when they showed that the T_1 of the anomeric proton of pyranose carbohydrates depends on the configuration¹². The T_1 is always longer when the proton is axial (Table 3). They ascribed this differential behaviour to different degrees of dipole-dipole relaxation that $\text{H}_{1\text{a}}$ and $\text{H}_{1\text{e}}$ have with $\text{H}_{3\text{a}}$ and $\text{H}_{5\text{a}}$. Sykes quantified the technique by using ^1H T_1 's to probe the solution geometry of *cis* and *trans*-crotonaldehyde¹³. His technique is based on applying equation (4) to determine the internuclear proton-proton distances. This approach requires two additional pieces of information. Firstly τ_{IS_j} needs to be known. This is available by measuring, as outlined above, the ^{13}C T_1 of a protonated carbon. To complete the analysis the percentage contribution of each proton to the relaxation time of the proton under study is required. This is available by measuring the $\text{H}_1\text{-H}_{\text{S}_j}$ nuclear Overhauser enhancements (NOE). A summary of NOE measurements on *cis* and *trans*-crotonaldehyde is given in Table 4 while a summary of the solution geometry as determined by ^1H T_1 studies for the *trans* isomer is given in Table 5. Here, a comparison is made with existing microwave data. It is apparent that some distances are determined accurately while for others the error is large. However, the technique does provide a way of obtaining structural information not accessible by other means.

TABLE 3 T_1 Values (in seconds) for the Anomeric Protons of Some Pyranose Carbohydrates.

Compound		$T_1(\text{H}_1 \text{ axial})$	$T_1(\text{H}_1 \text{ equatorial})$
D-Glucose	α		6.4
	β	3.4	
D-Galactose	α		7.0
	β	3.9	
D-Mannose	α		6.3
	β	1.8	
2-Acetamido-2-deoxy-D-glucopyranose	α		4.7
	β	2.3	
2-Acetamido-2-deoxy-D-mannopyranose	α		4.9
	β	1.1	

TABLE 3 Continued

Compound		$T_1(H_1 \text{ axial})$	$T_1(H_1 \text{ equatorial})$
Methyl D-glucopyranoside	α		2.4
	β	1.6	
Methyl D-xylopyranoside	α		3.8
	β	2.2	

TABLE 4 NOE Measurements for cis- and trans-Crotonaldehyde. The percentage increase is given.

Proton Irradiated	Proton Observed			
	a	m	r	x
a		4.4 (2.4)	0.8 (17.4)	4.7 (2.1)
m	1.5 (2.3)		23.3 (-2.0)	1.5 (3.8)
r	1.3 (25.7)	32.8 (4.0)		1.5
x	32.6 (0.1)	3.8 (24.2)	18.6 (11.6)	

() = trans results.

TABLE 5 NMR Determined Solution Geometry of trans-Crotonaldehyde.

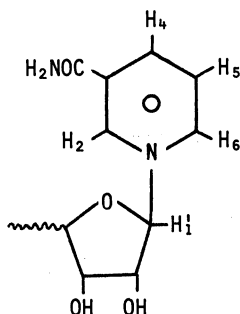
Separation Å	NMR	Microwave
a-m	3.66 ± 2.13 3.66 ± 0.95	3.13
a-r	2.37 ± 0.06 2.37 ± 0.08	2.31
m-r	3.32 ± 0.40	3.08
a-x	3.96 ± 0.67	4.71
m-x	3.04 ± 0.08	3.10
r-x	3.04 ± 0.14	2.90

Sykes' application of proton T_1 's to determine the solution geometry of crotonaldehyde required NOE measurements to determine the relative amounts of $H_I-H_{S_j}$ proton-proton relaxation. Ellis has also used proton relaxation studies to probe the solution structure of NAD^+ and NMN^+ but determined the relative amounts of $H_I-H_{S_j}$ proton relaxation by deuterium substitution¹⁴. Although this approach is theoretically more attractive it may, in general, be chemically unrealistic for many applications. The change in the T_1 of H_I from deuterium substitution for H_{S_j} is given by

$$\begin{aligned} \Delta\left(\frac{1}{T_1}\right) &= \frac{3}{2} \gamma_H^4 \hbar^2 \langle r_{IS_j}^{-6} \rangle \tau_c - \frac{8}{3} \gamma_D^2 \gamma_H^2 \hbar^2 \langle r_{ID_j}^{-6} \rangle \tau_c \\ &\approx \frac{3}{2} \gamma_H^4 \hbar^2 \langle r_{IS_j}^{-6} \rangle \tau_c \end{aligned} \quad (11)$$

Thus, $\langle r_{IS_j} \rangle$, the average value of the $I-S_j$ internuclear distance, can be readily determined. Ellis was interested in deducing whether the correct conformation of NAD^+ and NMN^+ was SYN or ANTI or whether the molecule was interconverting between the two forms. Evidence suggesting that it is a two state process is given in Table 6. It is clear that substituting either H_2 or H_6 with a deuterium has about the same effect on the T_1 of H_I thus the SYN or ANTI form are equally probable.

TABLE 6 Relaxation Times^a of the Pyridyl Protons of NAD^+ .^b



	H_2	H_4	H_5	H_6	H_I
NAD^+	0.41	0.66	0.40	0.28	0.32
NAD^+ H_2 -D					0.52
NAD^+ H_6 -D					0.42
NAD^+ $-H_2, H_6$ -D					0.75

^a T_1 is in seconds.

^bThe conformation of the SYN form is shown. The ANTI form is obtained by 180° rotation about the C_I-N bond.

Structural Applications of Other Relaxation Mechanisms

I wish to conclude this lecture by considering briefly one structural application of the quadrupolar and spin rotation relaxation mechanisms introduced above.

A very interesting application of spin rotation relaxation was provided by Ellis³. He and Zens showed that for CH_3-X compounds the spin rotational (SR) contribution to T_1 of CH_3 carbons can be approximated by

$$T_1(\text{SR}) = k_1 + k_2 V_0 \quad (12)$$

where k_1 and k_2 are constants and V_0 is the barrier height for rotation of the CH_3 group about the axis of the $\text{CH}_3\text{-X}$ bond. V_0 is in the most cases not accessible by conventional techniques. By separating the SR contribution to the observed T_1 by using the $^{13}\text{C}\text{-}^1\text{H}$ NOE as a measure of any dipole-dipole contribution, Ellis and Zens obtained the barrier heights listed in Table 7.

TABLE 7 Barrier Heights for $\text{CH}_3\text{-X}$ Bond Rotation Determined Experimentally from the Spin-Rotation Contribution to ^{13}C T_1 Values.

Compound	T_1^{a} (obs)	NOE	T_1^{a} (SR)	V_0^{b}
CH_3CN	20.4	1.46	26.5	0.09
$\text{CH}_3\text{C}\equiv\text{CCH}_3$	16.9	1.71	26.0	0.04
CH_3COOH	10.2	1.35	31.8	0.63
$(\text{CH}_3)_2\text{SiCl}_2$	13.5	1.42	49.7	2.46
$\text{CH}_3\text{CH}_2\text{I}$	16.1	1.47	61.7	3.69
CH_3CCl_3	12.5	1.67	78.0	5.36

^aIn seconds.

^bkcal/mole.

Lastly, it is clear from the above discussion that τ_C is a vital parameter in any quantitative study using T_1 values. As noted above the ^{13}C T_1 may be used to provide an experimental measurement of τ_C . ^2H T_1 may also be employed for this purpose because $\frac{e^2 Qq}{2h}$ is approximately constant for ^2H and τ_C may be computed using equation (6). As well, ^2H T_1 are affected by molecular structure and segmental motion. Data demonstrating the utility of such studies is summarized in Table 8¹⁵.

TABLE 8 Deuterium Spin-Lattice Relaxation Times^a (T_1) of Deuterated Compounds, in Carbon Tetrachloride Solution (5%) or as Neat Liquids.

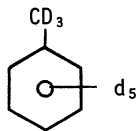
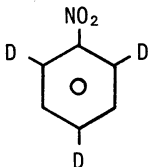
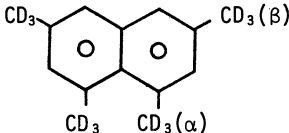
Compound	Group	T_1 (s)
	CD_3	4.3
	C-D(ar)	0.86
	C-D(o)	0.58
	C-D(p)	0.39
	$\text{CD}_3(\beta)$	0.91
	$\text{CD}_3(\alpha)$	0.24

TABLE 8 Continued

Compound	Group	T ₁ (s)
	CD ₃ (cis)	3.0
	CD ₃ (trans)	1.6
	CD	0.95

^aIn seconds.

I hope the above summary has high-lighted the potential that nuclear relaxation time measurements have in structural chemistry. I also hope I have managed to keep the discussion sufficiently simple and descriptive to tempt the practicing organic chemist and biochemist to use relaxation time measurements in solving structural problems.

REFERENCES

1. T.C. Farrar and E.D. Becker, "Pulse and Fourier Transform NMR", Academic Press, New York, 1971.
2. A. Allerhand, D. Doddrell, and R. Komoraski, *J.Chem.Phys.* **55**, 189 (1971).
3. A.P. Zens and P.D. Ellis, *J.Am.Chem.Soc.* **97**, 5685 (1975).
4. D.M. Doddrell, D.T. Pegg, M.R. Bendall, and A.K. Gregson, *Chem.Phys.Letts.* **40**, 142 (1976).
5. D.M. Doddrell and A. Allerhand, *J.Am.Chem.Soc.* **93**, 1558 (1976).
6. A. Allerhand and D.M. Doddrell, *J.Am.Chem.Soc.* **93**, 2779 (1971); A. Allerhand, D. Doddrell, and R. Komoraski, *J.Chem.Phys.* **55**, 189 (1971).
7. P. Barron, unpublished results.
8. A. Allerhand, D. Doddrell, V. Glushko, D.W. Cochran, E. Wenkert, P.J. Lawson, and F.R.N. Gurd, *J.Am.Chem.Soc.* **93**, 544 (1971).
9. E. Oldfield and A. Allerhand, *J.Am.Chem.Soc.* **97**, 221 (1975); E. Oldfield, R.S. Norton, and A. Allerhand, *J.Biol.Chem.* **250**, 6368 (1975); **250**, 6381 (1975).
10. R.A. Dwek, "Nuclear Magnetic Resonance in Biochemistry", Clarendon Press, Oxford, 1973.
11. C.F. Brewer, H. Sternlicht, D.M. Marcus, and A.P. Grolman, *Biochemistry* **12** 4448 (1973).
12. L.D. Hall and C. Preston, *J.Chem.Soc., Chem.Comm.*, 1319 (1972).
13. R. Roman III, J.A. McCammon, and B.D. Sykes, *J.Am.Chem.Soc.* **96**, 4773 (1974).
14. A.P. Zens, T.J. Williams, J.C. Wisowaty, R.R. Fisher, R.B. Dunlap, T.A. Bryson, and P.D. Ellis, *J.Am.Chem.Soc.* **97**, 2850 (1975).
15. H.H. Mantsch, H. Saito, L.C. Leitch, and I.C.P. Smith, *J.Am.Chem.Soc.* **96**, 256 (1974).